NASA/TM—2008-215490

Atomic Oxygen Erosion Yield Predictive Tool for Spacecraft Polymers in Low Earth Orbit

Bruce A. Banks
Alphaport, Inc., Cleveland, Ohio

Jane A. Backus
Ohio Aerospace Institute, Brook Park, Ohio

Kim K. de Groh
Glenn Research Center, Cleveland, Ohio

December 2008

NASA STI Program . . . in Profile

Since its founding, NASA has been dedicated to the advancement of aeronautics and space science. The NASA Scientific and Technical Information (STI) program plays a key part in helping NASA maintain this important role.

The NASA STI Program operates under the auspices of the Agency Chief Information Officer. It collects, organizes, provides for archiving, and disseminates NASA's STI. The NASA STI program provides access to the NASA Aeronautics and Space Database and its public interface, the NASA Technical Reports Server, thus providing one of the largest collections of aeronautical and space science STI in the world. Results are published in both non-NASA channels and by NASA in the NASA STI Report Series, which includes the following report types:

- TECHNICAL PUBLICATION. Reports of completed research or a major significant phase of research that present the results of NASA programs and include extensive data or theoretical analysis. Includes compilations of significant scientific and technical data and information deemed to be of continuing reference value. NASA counterpart of peer-reviewed formal professional papers but has less stringent limitations on manuscript length and extent of graphic presentations.

- TECHNICAL MEMORANDUM. Scientific and technical findings that are preliminary or of specialized interest, e.g., quick release reports, working papers, and bibliographies that contain minimal annotation. Does not contain extensive analysis.

- CONTRACTOR REPORT. Scientific and technical findings by NASA-sponsored contractors and grantees.

- CONFERENCE PUBLICATION. Collected papers from scientific and technical conferences, symposia, seminars, or other meetings sponsored or cosponsored by NASA.

- SPECIAL PUBLICATION. Scientific, technical, or historical information from NASA programs, projects, and missions, often concerned with subjects having substantial public interest.

- TECHNICAL TRANSLATION. English-language translations of foreign scientific and technical material pertinent to NASA's mission.

Specialized services also include creating custom thesauri, building customized databases, organizing and publishing research results.

For more information about the NASA STI program, see the following:

- Access the NASA STI program home page at *http://www.sti.nasa.gov*

- E-mail your question via the Internet to *help@sti.nasa.gov*

- Fax your question to the NASA STI Help Desk at 301–621–0134

- Telephone the NASA STI Help Desk at 301–621–0390

- Write to:
  NASA Center for AeroSpace Information (CASI)
  7115 Standard Drive
  Hanover, MD 21076–1320

NASA/TM—2008-215490

Atomic Oxygen Erosion Yield Predictive Tool for Spacecraft Polymers in Low Earth Orbit

Bruce A. Banks
Alphaport, Inc., Cleveland, Ohio

Jane A. Backus
Ohio Aerospace Institute, Brook Park, Ohio

Kim K. de Groh
Glenn Research Center, Cleveland, Ohio

National Aeronautics and
Space Administration

Glenn Research Center
Cleveland, Ohio 44135

December 2008

Level of Review: This material has been technically reviewed by technical management.

Available from

NASA Center for Aerospace Information
7115 Standard Drive
Hanover, MD 21076–1320

National Technical Information Service
5285 Port Royal Road
Springfield, VA 22161

Available electronically at http://gltrs.grc.nasa.gov

Atomic Oxygen Erosion Yield Predictive Tool for Spacecraft Polymers in Low Earth Orbit

Bruce A. Banks
Alphaport, Inc.
Cleveland, Ohio 44135

Jane A. Backus
Ohio Aerospace Institute
Brook Park, Ohio 44142

Kim K. de Groh
National Aeronautics and Space Administration
Glenn Research Center
Cleveland, Ohio 44135

Abstract

A predictive tool was developed to estimate the low Earth orbit (LEO) atomic oxygen erosion yield of polymers based on the results of the Polymer Erosion and Contamination Experiment (PEACE) Polymers experiment flown as part of the Materials International Space Station Experiment 2 (MISSE 2). The MISSE 2 PEACE experiment accurately measured the erosion yield of a wide variety of polymers and pyrolytic graphite. The 40 different materials tested were selected specifically to represent a variety of polymers used in space as well as a wide variety of polymer chemical structures. The resulting erosion yield data was used to develop a predictive tool which utilizes chemical structure and physical properties of polymers that can be measured in ground laboratory testing to predict the in-space atomic oxygen erosion yield of a polymer. The properties include chemical structure, bonding information, density and ash content. The resulting predictive tool has a correlation coefficient of 0.914 when compared with actual MISSE 2 space data for 38 polymers and pyrolytic graphite. The intent of the predictive tool is to be able to make estimates of atomic oxygen erosion yields for new polymers without requiring expensive and time consumptive in-space testing.

1.0 Introduction

Hydrocarbon polymers exposed to the LEO environment during the early space Shuttle flights were found to gradually erode away as a result of atomic oxygen exposure, as the atomic oxygen interacted with the polymers causing the surface to convert to volatile oxidation products. It soon became apparent that not all polymers experienced oxidative erosion at the same rate (refs. 1 to 6). The measure of a polymer's susceptibility to atomic oxygen erosion is the atomic oxygen erosion yield, which is the volume lost per incident atomic oxygen atom, given in cm^3/atom (ref. 7). Numerous LEO flight experiments have been performed that have contributed to the available data on atomic oxygen erosion yields for a variety of materials. Many of these experiments were conducted on various short duration shuttle missions including STS–5 (ref. 1), STS–8 (ref. 8), and the Evaluation of Oxygen Interactions with Materials-3 (EOIM–3) experiment on STS–46 (ref. 10). In addition, many materials were evaluated after 5.8 yr of LEO exposure on the Long Duration Exposure Facility (LDEF) (ref. 9). Unfortunately, many of the early experiments did not utilize dehydrated mass loss measurements, and the resulting mass loss due to atomic oxygen exposure may have been obscured because samples were often not in consistent states of dehydration during the pre-flight and post-flight mass measurements. This is a particular problem for short duration mission exposures or low erosion yield materials.

The MISSE 2 PEACE Polymers experiment used carefully dehydrated mass measurements, as well as accurate density measurements and an error analysis to obtain accurate high fluence (a 4 yr exposure with an atomic oxygen fluence of 8.43×10^{21} atoms/cm^2) erosion yield data for 40 polymers and pyrolytic graphite (refs. 11 and 12).

The MISSE 2 PEACE materials were selected specifically to represent a variety of polymers used in space as well as a wide variety of polymer chemical structures. The intent of the variety of polymer structures was to use the data to assist in the development of an atomic oxygen erosion yield predictive tool, which would allow the prediction of LEO erosion yields of new polymers based on chemical structure and simple low-cost ground laboratory test data rather than requiring actual in-space LEO testing for every new polymer that is developed. An erosion yield predictive tool has been developed based on the MISSE 2 PEACE experiment and is described in this paper.

As LEO erosion yield data gradually became available, it was noticed that some polymers, such as the fluoropolymers had low erosion yields compared to polyimide Kapton H, and others that contain significant amounts of bonded oxygen such as polycarbonate had higher erosion yields than Kapton H. The dependence of atomic oxygen erosion yield on chemical structure has been explored based on early available LEO data (refs. 13 to 15). The formula developed, and described in this paper, is based on best fit criteria to the MISSE 2 PEACE spaceflight data (ref. 12). The predictive tool is applicable to all polymers that contain any of the following elements: carbon, hydrogen, nitrogen, oxygen, fluorine, chlorine and sulfur.

2.0 Atomic Oxygen Predictive Tool Development

The modeling information used to develop an atomic oxygen predictive tool consisted of using the MISSE 2 PEACE Polymers LEO atomic oxygen erosion yield data from references 11 and 12, polymer chemical structure information concerning the number and types of chemical bonds, polymer density information, and fractional ash content data. The atomic oxygen predictive tool was developed using these properties and assuming an unknown degree of dependence which was tuned to the highest correlation between actual LEO results and the predictive tool. Thus, for every physical property or chemical bond type, a degree of dependence was assumed which was optimized to provide the closest match between predicted and actual erosion yields.

2.1 LEO Atomic Oxygen Erosion Yield Data

Atomic oxygen erosion yield data was obtained from the MISSE 2 PEACE Polymers experiment, which exposed 41 one inch diameter samples, including two Kapton H polyimide atomic oxygen fluence witness samples. This experiment was flown in MISSE Passive Experiment Carrier 2 (PEC 2), tray 1 which was attached on the exterior of the International Space Station Quest Airlock. This experiment was exposed to atomic oxygen along with solar and charged particle radiation. The experiment was exposed to the LEO environment for 3.95 yr from August 16, 2001 to July 30, 2005, and successfully retrieved during a space walk on July 30, 2005 during Discovery's STS–114 Return to Flight mission. Figure 1 shows MISSE 2 on the International Space Station. Figures 2 and 3 show pre- and post-flight photos of the MISSE 2 PEACE Polymers experiment tray containing the 40 polymers and pyrolytic graphite.

The 40 different materials (41 samples) tested included those commonly used for spacecraft applications, such as Teflon FEP (DuPont), to more recently developed polymers, such as high temperature polyimide PMR–15 (polymerization of monomer reactants), and pyrolytic graphite.

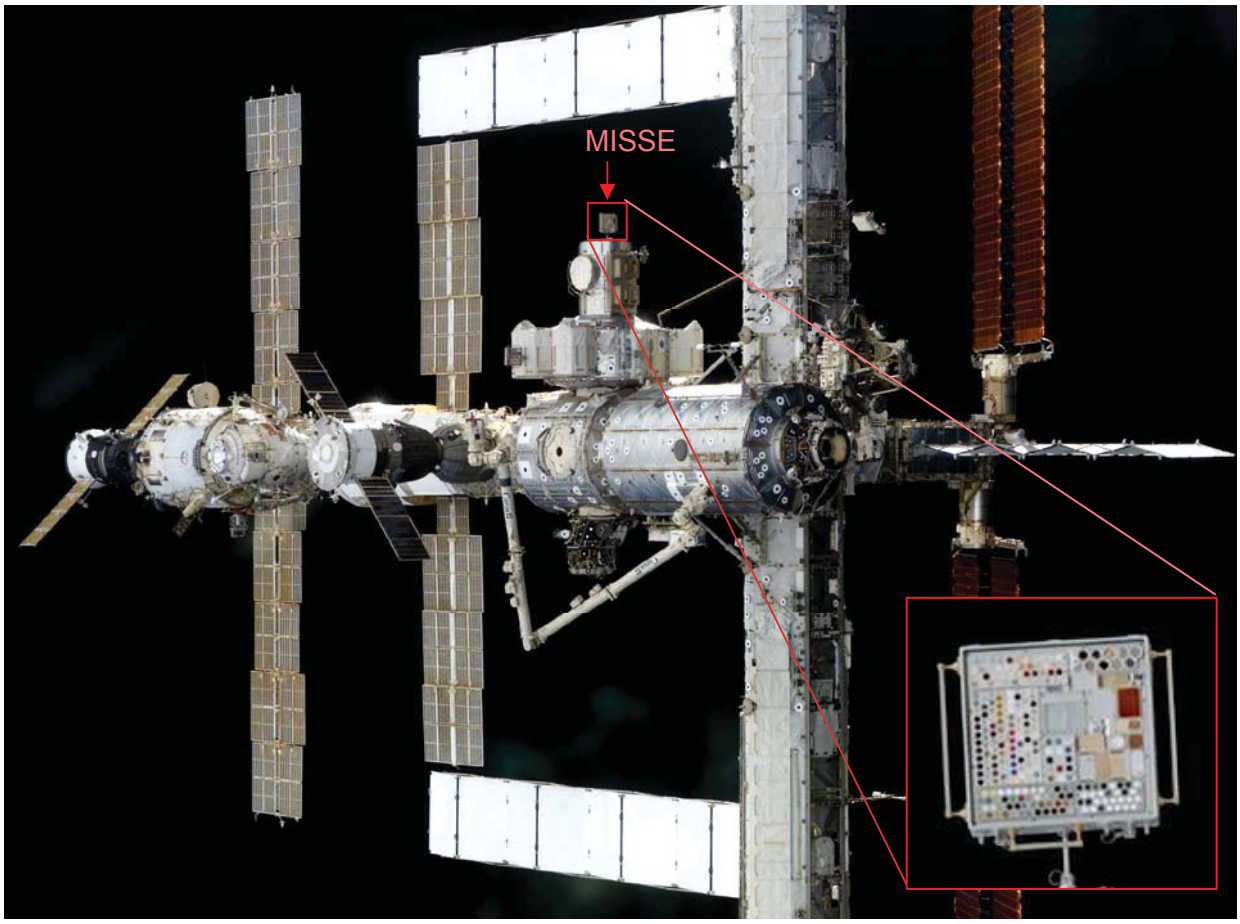

Figure 1.—MISSE 2 Passive Experiment Carrier 2 Tray 1 holding the PEACE polymers attached to the International Space Station August 16, 2001 to July 30, 2005.

Figure 2.—Photograph of the MISSE 2 PEACE Polymers experiment prior to flight. The labels shown on the samples are defined in table 1.

Figure 3.—Photograph of the MISSE 2 PEACE Polymers experiment post-flight.

Details of the specific polymers flown, flight sample fabrication, solar and ionizing radiation environmental exposure, pre-flight and post-flight characterization techniques, and atomic oxygen fluence calculations are presented in references 11 and 12. Additional details on environmental exposure are provided by Pippin in reference 17. The atomic oxygen fluence was found to be 8.43×10^{21} atoms/cm^2 based on the average of the two fluence witness samples. The total equivalent sun hours (ESH) was estimated to be 5,000 to 6,700 ESH. This total includes Earth-reflected illumination (650 to 820 ESH). The base-plate thermal cycling temperature range for MISSE 2 was nominally between 40 and –30 °C with occasional short-term excursions to more extreme temperatures (ref. 17). Results of x-ray photoelectron spectroscopy (XPS) contamination analysis of two MISSE 2 sapphire witness samples in tray E6 (located on the same MISSE surface and next to tray E5) indicated the space experiment had received very little contamination. An extremely thin silica contaminant layer of 1.3 and 1.4 nm was on each slide, respectively (ref. 18).

The MISSE 2 PEACE Polymers LEO atomic oxygen erosion yield data, which was used for the predictive tool is given in table I (refs. 11 and 12). In some cases, the erosion yield is greater than the value listed because a portion or all of the exposed area of the flight sample was completely eroded through all layers (many samples were stacked thin film polymers). In these cases, the measured erosion yields were also included in the data set to develop a predictive erosion yield equation because, in general, the samples appeared that they eroded partially or completely through at a fluence level close to the full mission fluence.

TABLE I.—MISSE 2 PEACE POLYMERS EROSION YIELD DATA

Material	Polymer abbreviation	MISSE 2 erosion yield, cm^3/atom
Acrylonitrile butadiene styrene	ABS	1.09×10^{-24}
Cellulose acetate	CA	5.05×10^{-24}
Poly-(p-phenylene terephthalamide)	PPDT (Kevlar)	6.28×10^{-25}
Polyethylene	PE	$>3.74\times10^{-24}$
Polyvinyl fluoride	PVF (clear Tedlar)	3.19×10^{-24}
Crystalline polyvinylfluoride with white pigment	PVF (white Tedlar)	1.01×10^{-25}
Polyoxymethylene; acetal; polyformaldehyde	POM (Delrin)	9.14×10^{-24}
Polyacrylonitrile	PAN	1.41×10^{-24}
Allyl diglycol carbonate	ADC (CR–39)	$>6.80\times10^{-24}$
Polystyrene	PS	3.74×10^{-24}
Polymethyl methacrylate	PMMA	$>5.60\times10^{-24}$
Polyethylene oxide	PEO	1.93×10^{-24}
Poly(p-phenylene-2 6-benzobisoxazole)	PBO (Zylon)	1.36×10^{-24}
Epoxide or epoxy	EP	4.21×10^{-24}
Polypropylene	PP	2.68×10^{-24}
Polybutylene terephthalate	PBT	9.11×10^{-24}
Polysulphone	PSU	2.94×10^{-24}
Polyurethane	PU	1.56×10^{-24}
Polyphenylene isophthalate	PPPA (Nomex)	1.41×10^{-24}
Pyrolytic graphite	PG	4.15×10^{-25}
Polyetherimide	PEI	$>3.31\times10^{-24}$
Polyamide 6 or nylon 6	PA 6	3.51×10^{-24}
Polyamide 66 or nylon 66	PA 66	1.80×10^{-24}
Polyimide	PI (CP1)	1.91×10^{-24}
Polyimide (PMDA)	PI (Kapton H)	3.00×10^{-24}
Polyimide (PMDA)	PI (Kapton HN)	2.81×10^{-24}
Polyimide (BPDA)	PI (Upilex–S or US)	9.22×10^{-24}
High temperature polyimide resin	PI (PMR–15)	$>3.02\times10^{-24}$
Polybenzimidazole	PBI	$>2.21\times10^{-24}$
Polycarbonate	PC	4.29×10^{-24}
Polyetheretherkeytone	PEEK	2.99×10^{-24}
Polyethylene terephthalate	PET (Mylar)	3.01×10^{-24}
Chlorotrifluoroethylene	CTFE (Kel–f)	8.31×10^{-25}
Ethylene-chlorotrifluoroethylene	ECTFE (Halar)	1.79×10^{-24}
Tetrafluorethylene-ethylene copolymer	ETFE (Tefzel)	9.61×10^{-25}
Fluorinated ethylene propylene	FEP	2.00×10^{-25}
Polytetrafluoroethylene	PTFE	1.42×10^{-25}
Perfluoroalkoxy copolymer resin	PFA	1.73×10^{-25}
Amorphous Fluoropolymer	AF	1.98×10^{-25}
Polyvinylidene fluoride	PVDF (Kynar)	1.29×10^{-24}

2.2 Polymer Physical Properties

Polymer density information was obtained from either supplier information or density gradient column testing (described in ref. 12).

Most polymers contain some fraction of inorganic material. As atomic oxygen erodes a polymer that contains inorganic material, the resulting nonvolatile ash begins to accumulate on the eroded surface of the polymer. For high fluence missions, such as for the MISSE 2 PEACE polymers where the fluence was 8.43×10^{21} atoms/cm^2 (ref. 19), this can cause the atomic oxygen to gradually become somewhat shielded from reacting with the underlying polymer. As a result, it is believed that the ash content of polymers can have an influence on the erosion yield of a polymer. If one compares the erosion yield of clear polyvinyl fluoride (clear Tedlar (DuPont)) with that of white Tedlar one can see that the titanium dioxide pigment in white Tedlar shields the Tedlar resulting in the very different erosion yields of $3.19\times10^{-24}cm^3$/atom and $0.101\times10^{-24}cm^3$/atom, respectively.

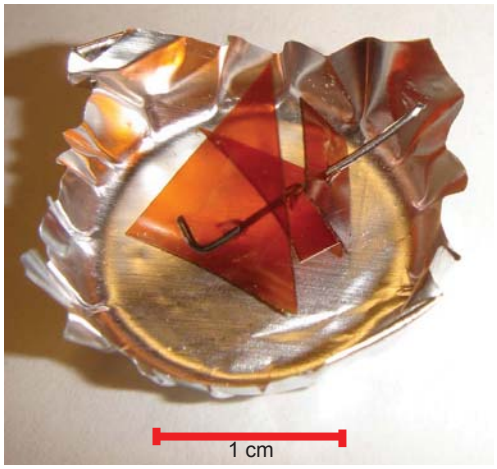

Figure 4.—Polymer sample in aluminum cup with platinum wire weighting it down for ash content evaluation using an RF plasma asher.

Ash content described in this paper is the fraction of the initial dehydrated polymer mass that is nonvolatile and remains as an ash after the polymer has been completely oxidized. This was determined by placing pieces of each polymer in thin (0.00254 mm thick) aluminum foil cups, placing short platinum wires through the samples (see fig. 4), and ashing them for several hundred hours in a RF plasma asher operated on air (ref. 16) until only an ash and no polymer remained. The aluminum foil cups were previously exposed to atomic oxygen to remove organic coatings that typically reside on aluminum foil as a result of foil processing. The purpose of the platinum wires was to prevent the resulting light and fragile ash from blowing away as the sample was transported from the asher to a Mettler microgram sensitivity microbalance.

Table II lists the density, ρ, and mass fraction of the polymer that is ash, N_a, measured for each of the MISSE PEACE polymers. The ash content is a difficult measurement to accurately make because the ash is too fragile and easily blown away with the slightest of air flow. As a result, the uncertainty of many of the ash measurements may be significant, and is unknown at the current time.

2.3 Polymer Chemical Structure

The chemical structure for each of the polymers and pyrolytic graphite is given in appendix A. The minimum volume of a repeat unit was calculated to allow a comparison of how densely the atoms theoretically could be packed in comparison to the actual case where larger spaces would occur between atoms where van der Waals bonding exists or void spaces exits. Such a ratio is a comparison of how densely those atoms are packed. Loosely packed atoms should result in a high erosion yield compared to densely packed atoms. The minimum volume of the atoms that make up a polymer repeat unit was based on the sum of the atoms making up the polymer repeat unit assuming each atoms volume is determined by its covalent radii. Table III lists the covalent radii of the various types of atoms in the MISSE 2 PEACE polymer experiment.

TABLE II.—MISSE 2 PEACE POLYMERS DENSITY AND FRACTIONAL ASH CONTENT

Material	Polymer abbreviation	Density, ref. 12, ρ, g/cm^3	Mass fraction of polymer that is ash, N_a
Acrylonitrile butadiene styrene	ABS	1.05	4.58×10^{-2}
Cellulose acetate	CA	1.2911	2.83×10^{-3}
Poly-(p-phenylene terephthalamide)	PPDT (Kevlar)	1.4422	3.72×10^{-3}
Polyethylene	PE	0.918	2.03×10^{-2}
Polyvinyl fluoride	PVF (Clear Tedlar)	1.3792	1.36×10^{-1}
Crystalline polyvinylfluoride with white pigment	PVF (White Tedlar)	1.6241	2.90×10^{-1}
Polyoxymethylene; acetal; polyformaldehyde	POM (Delrin)	1.3984	9.02×10^{-3}
Polyacrylonitrile	PAN	1.1435	1.84×10^{-3}
Allyl diglycol carbonate	ADC (CR–39)	1.3173	2.65×10^{-3}
Polystyrene	PS	1.0503	4.20×10^{-4}
Polymethyl methacrylate	PMMA	1.1628	2.80×10^{-4}
Polyethylene oxide	PEO	1.1470	1.12×10^{-3}
Poly(p-phenylene-2 6-benzobisoxazole)	PBO (Zylon)	1.3976	1.09×10^{-2}
Epoxide or epoxy	EP	1.1150	3.34×10^{-2}
Polypropylene	PP	0.9065	1.84×10^{-3}
Polybutylene terephthalate	PBT	1.3318	6.29×10^{-2}
Polysulphone	PSU	1.2199	3.48×10^{-3}
Polyurethane	PU	1.2345	6.64×10^{-3}
Polyphenylene isophthalate	PPPA (Nomex)	0.72	4.76×10^{-2}
Pyrolytic graphite	PG	2.22	1.54×10^{-3}
Polyetherimide	PEI	1.2873	1.05×10^{-3}
Polyamide 6 or nylon 6	PA 6	1.1233	1.12×10^{-3}
Polyamide 66 or nylon 66	PA 66	1.2252	3.61×10^{-3}
Polyimide	PI (CP1)	1.4193	1.71×10^{-3}
Polyimide (PMDA)	PI (Kapton H)	1.4273	2.25×10^{-3}
Polyimide (PMDA)	PI (Kapton HN)	1.4345	4.41×10^{-3}
Polyimide (BPDA)	PI (Upilex–S or US)	1.3866	4.82×10^{-4}
High temperature polyimide resin	PI (PMR–15)	1.3232	9.27×10^{-4}
Polybenzimidazole	PBI	1.2758	9.92×10^{-4}
Polycarbonate	PC	1.1231	1.77×10^{-3}
Polyetheretherkeytone	PEEK	1.2259	8.26×10^{-3}
Polyethylene terephthalate	PET (Mylar)	1.3925	2.04×10^{-3}
Chlorotrifluoroethylene	CTFE (Kel–f)	2.1327	6.55×10^{-4}
Ethylene-chlorotrifluoroethylene	ECTFE (Halar)	1.6761	1.23×10^{-3}
Tetrafluorethylene-ethylene copolymer	ETFE (Tefzel)	1.7397	5.34×10^{-3}
Fluorinated ethylene propylene	FEP	2.1443	4.27×10^{-2}
Polytetrafluoroethylene	PTFE	2.1503	2.98×10^{-4}
Perfluoroalkoxy copolymer resin	PFA	2.1383	3.62×10^{-2}
Amorphous fluoropolymer	AF	2.1463	3.58×10^{-2}
Polyvinylidene fluoride	PVDF (Kynar)	1.7623	4.68×10^{-2}

TABLE III.—COVALENT RADII OF ATOMS USED IN THE MISSE 2 PEACE POLYMER EXPERIMENT

Atom	Covalent radii, cm
Carbon	7.70×10^{9}
Hydrogen	3.70
Oxygen	7.30
Nitrogen	7.50
Fluorine	7.10
Chlorine	9.90
Sulfur	1.02×10^{8}

The formula for the smallest repeat unit of each polymer, the atomic mass units (AMU) for the repeat unit, the volume for each repeat unit (V_r), and the predicted minimum volume of a repeat unit, V_Σ, which is based on the sum of the volume of each atom using the covalent radii of atoms in the repeat unit is listed in table IV. Some of the repeat units are sufficiently complex that formulas have been rounded to the closest integer for the number of atoms of each type. The volume of each repeat unit was determined based on the chemical structure of the repeat unit (shown in appendix A) as well as the molecular weight and density of the material. Thus, if the ratio of V_Σ/V_r was much less than one, then one would expect the erosion yield to be higher than similarly structured polymers where the atoms are packed closer together.

The predictive tool also uses the number atoms, and the chemical bonds of each type (element-to-carbon atom and single, double or triple bond) per carbon atom in the repeat unit because both appear to influence the erosion yield of the polymers. Table V lists the number of atoms of various types for each polymer.

TABLE IV.—MISSE 2 PEACE POLYMERS CHEMICAL STRUCTURE

Material	Polymer abbreviation	Formula	Atomic mass units, g/mole	Volume per repeat unit, V_r, cm^3	Minimum volume of atoms in repeat unit, V_Σ, cm^3
Acrylonitrile butadiene styrene	ABS	$C_{23}H_{23}N$	313.4414	4.99×10^{-22}	5.11×10^{-23}
Cellulose acetate	CA	$C_{12}H_{16}O_8$	288.2536	3.64×10^{-22}	3.83×10^{-23}
Poly-(p-phenylene terephthalamide)	PPD–T (Kevlar)	$C_{14}H_{10}N_2O_2$	238.2452	2.74×10^{-22}	3.57×10^{-23}
Polyethylene	PE	C_2H_4	28.0536	5.07×10^{-23}	4.67×10^{-24}
Polyvinyl fluoride, clear	PVF (Tedlar)	C_2H_3F	46.0437	5.54×10^{-23}	5.96×10^{-24}
Polyvinyl fluoride, white pigment	PVF (W. Tedlar)	C_2H_3F	46.0437	5.54×10^{-23}	5.96×10^{-24}
Polyoxymethylene; acetal; polyformaldehyde	POM (Delrin)	CH_2O	30.0262	3.57×10^{-23}	3.97×10^{-24}
Polyacrylonitrile	PAN	C_3H_3N	53.0634	7.71×10^{-23}	8.14×10^{-24}
Allyl diglycol carbonate	ADC (CR–39)	$C_{12}H_{18}O_7$	274.2700	3.46×10^{-22}	3.82×10^{-23}
Polystyrene	PS	C_8H_8	104.1512	1.65×10^{-22}	1.70×10^{-23}
Polymethyl methacrylate	PMMA	$C_5H_8O_2$	100.1170	1.43×10^{-22}	1.45×10^{-23}
Polyethylene oxide	PEO	C_2H_4O	44.0530	6.38×10^{-23}	6.30×10^{-24}
Poly(p-phenylene-2 6-benzobisoxazole)	PBO (Zylon)	$C_{14}H_6N_2O_2$	258.2356	3.07×10^{-22}	3.48×10^{-23}
Epoxide or epoxy	EP	$C_{20}H_{19}O_3$	307.3683	9.30×10^{-22}	9.53×10^{-23}
Polypropylene	PP	C_3H_6	42.0804	7.71×10^{-23}	7.01×10^{-24}
Polybutylene terephthalate	PBT	$C_{12}H_{12}O_4$	220.2244	2.75×10^{-22}	3.20×10^{-23}
Polysulphone	PSU	$C_{27}H_{22}O_4S$	442.5344	6.02×10^{-22}	6.73×10^{-23}
Polyurethane	PU	$C_6H_{10}O_4N_2$	174.1560	2.34×10^{-22}	2.36×10^{-23}
Polyphenylene isophthalate	PPPA (Nomex)	$C_{14}H_{10}O_2N_2$	238.2452	5.49×10^{-22}	3.57×10^{-23}
Pyrolytic graphite	PG	C_6	72.0660	5.39×10^{-23}	1.15×10^{-23}
Polyetherimide	PEI	$C_{37}H_{24}O_6N_2$	592.6064	7.64×10^{-22}	8.92×10^{-23}
Polyamide 6 or nylon 6	PA 6	$C_6H_{11}NO$	113.1590	1.67×10^{-22}	1.72×10^{-23}
Polyamide 66 or nylon 66	PA 66	$C_{12}H_{22}N_2O_2$	226.3180	3.07×10^{-22}	3.44×10^{-23}
Polyimide	PI (CP1)	$C_{46}H_{22}O_6N_2F_{12}$	926.6656	1.08×10^{-21}	1.24×10^{-22}
Polyimide (PMDA)	PI (Kapton H)	$C_{22}H_{10}O_5N_2$	382.3314	4.45×10^{-22}	5.59×10^{-23}
Polyimide (PMDA)	PI (Kapton HN)	$C_{22}H_{10}O_5N_2$	382.3314	4.43×10^{-22}	5.59×10^{-23}
Polyimide (BPDA)	PI (Upilex–S)	$C_{22}H_{10}O_4N_2$	366.3320	4.39×10^{-22}	5.42×10^{-23}
High temperature polyimide resin	PI (PMR–15)	$C_{95}H_{57}O_{14}N_6$	1506.5271	1.79×10^{-21}	2.14×10^{-22}
Polybenzimidazole	PBI	$C_{20}H_{12}N_4$	308.3416	4.01×10^{-22}	4.79×10^{-23}
Polycarbonate	PC	$C_{16}H_{14}O_3$	254.2848	3.76×10^{-22}	3.85×10^{-23}
Polyetheretherkeytone	PEEK	$C_{19}H_{12}O_2$	272.3026	3.69×10^{-22}	4.21×10^{-23}
Polyethylene terephthalate	PET (Mylar)	$C_{10}H_8O_4$	192.1708	2.29×10^{-22}	2.73×10^{-23}
Chlorotrifluoroethylene	CTFE (Kel–f)	C_2ClF_3	116.4687	9.07×10^{-23}	8.32×10^{-24}
Halar ethylene-chlorotrifluoroethylene	ECTFE (Halar)	$C_4H_4ClF_3$	144.5223	1.43×10^{-22}	1.71×10^{-23}
Tetrafluorethylene-ethylene copolymer	ETFE (Tefzel)	$C_4H_4F_4$	128.0676	1.22×10^{-22}	1.45×10^{-23}
Fluorinated ethylene propylene	FEP	C_6F_{12}	300.0420	2.32×10^{-22}	2.95×10^{-23}
Polytetrafluoroethylene	PTFE	C_2F_4	100.0140	7.72×10^{-23}	9.82×10^{-24}
Perfluoroalkoxy copolymer resin	PFA	$C_{203}OF_{406}$	10167.4204	7.90×10^{-21}	9.99×10^{-22}
Amorphous fluoropolymer	AF	$C_{19}O_6F_{32}$	932.1414	7.21×10^{-22}	9.41×10^{-23}
Polyvinylidene fluoride	PVDF (Kynar)	$C_2H_2F_2$	64.0338	6.03×10^{-23}	5.11×10^{-23}

TABLE V.—THE NUMBER OF ATOMS OF VARIOUS TYPES FOR EACH MISSE 2 PEACE POLYMER

Material	Polymer abbreviation	Formula	Number of atoms in repeat unit							
			N_C	N_H	N_O	N_N	N_S	N_{Cl}	N_F	Total, N_t
Acrylonitrile butadiene styrene	ABS	$C_{23}H_{25}N$	23	25	0	1	0	0	0	47
Cellulose acetate	CA	$C_{12}H_{16}O_8$	12	16	8	0	0	0	0	36
Poly-(p-phenylene terephthalamide)	PPD–T (Kevlar)	$C_{14}H_{10}N_2O_2$	14	10	2	2	0	0	0	28
Polyethylene	PE	C_2H_4	2	4	0	0	0	0	0	6
Polyvinyl fluoride	PVF (Clear Tedlar)	C_2H_3F	2	3	0	0	0	0	1	6
Crystalline polyvinylfluoride with white pigment	PVF (White Tedlar)	C_2H_3F	2	3	0	0	0	0	1	6
Polyoxymethylene; acetal; polyformaldehyde	POM (Delrin)	CH_2O	1	2	1	0	0	0	0	4
Polyacrylonitrile	PAN	C_3H_3N	3	3	0	1	0	0	0	7
Allyl diglycol carbonate	ADC (CR–39)	$C_{12}H_{18}O_7$	12	18	7	0	0	0	0	37
Polystyrene	PS	C_8H_8	8	8	0	0	0	0	0	16
Polymethyl methacrylate	PMMA	$C_5H_8O_2$	5	8	2	0	0	0	0	15
Polyethylene oxide	PEO	C_2H_4O	2	4	1	0	0	0	0	7
Poly-(p-phenylene-2 6-benzobisoxazole)	PBO (Zylon)	$C_{14}H_6N_2O_2$	14	6	2	2	0	0	0	24
Epoxide or epoxy	EP	$C_{39}H_{44}O_7$	20	19	3	0	0	0	0	42
Polypropylene	PP	C_3H_6	3	6	0	0	0	0	0	9
Polybutylene terephthalate	PBT	$C_{12}H_{12}O_4$	12	12	4	0	0	0	0	28
Polysulphone	PSU	$C_{27}H_{22}O_4S$	27	22	4	0	1	0	0	54
Polyurethane	PU	$C_6H_{10}O_4N_2$	6	10	4	2	0	0	0	22
Polyphenylene isophthalate	PPPA (Nomex)	$C_{14}H_{10}O_2N_2$	14	10	2	2	0	0	0	28
Pyrolytic graphite	PG	C_6	6	0	0	0	0	0	0	6
Polyetherimide	PEI	$C_{37}H_{24}O_6N_2$	37	24	6	2	0	0	0	69
Polyamide 6 or nylon 6	PA 6	$C_6H_{11}NO$	6	11	1	1	0	0	0	19
Polyamide 66 or nylon 66	PA 66	$C_{12}H_{22}N_2O_2$	12	22	2	2	0	0	0	38
Polyimide	PI (CP1)	$C_{46}H_{22}O_6N_2F_{12}$	46	22	6	2	0	0	12	88
Polyimide (BPDA)	PI (Kapton H)	$C_{22}H_{10}O_5N_2$	22	10	5	2	0	0	0	39
Polyimide (PMDA)	PI (Kapton HN)	$C_{22}H_{10}O_5N_2$	22	10	5	2	0	0	0	39
Polyimide (PMDA)	PI (Upilex–S)	$C_{22}H_{10}O_4N_2$	22	10	4	2	0	0	0	38
High temperature polyimide resin	PI (PMR–15)	$C_{95}H_{57}O_{14}N_6$	95	57	14	6	0	0	0	172
Polybenzimidazole	PBI	$C_{20}H_{12}N_4$	20	12	0	4	0	0	0	36
Polycarbonate	PC	$C_{16}H_{14}O_3$	16	14	3	0	0	0	0	33
Polyetheretherkeytone	PEEK	$C_{19}H_{12}O_2$	19	12	2	0	0	0	0	33
Polyethylene terephthalate	PET (Mylar)	$C_{10}H_8O_4$	10	8	4	0	0	0	0	22
Chlorotrifluoroethylene	CTFE (Kel–f)	C_2ClF_3	2	0	0	0	0	1	3	6
Ethylene-chlorotrifluoroethylene	ECTFE (Halar)	$C_4H_4ClF_3$	4	4	0	0	0	1	3	12
Tetrafluorethylene-ethylene copolymer	ETFE (Tefzel)	$C_4H_4F_4$	4	4	0	0	0	0	4	12
Fluorinated ethylene propylene	FEP	$C_{11}F_{22}$	11	0	0	0	0	0	22	33
Polytetrafluoroethylene	PTFE	C_2F_4	2	0	0	0	0	0	4	6
Perfluoroalkoxy copolymer resin	PFA	$C_{203}OF_{406}$	203	0	1	0	0	0	406	610
Amorphous fluoropolymer	AF	$C_{19}O_6F_{32}$	19	0	6	0	0	0	32	57
Polyvinylidene fluoride	PVDF (Kynar)	$C_2H_2F_2$	2	2	0	0	0	0	2	6

Where

N_C Number of carbon atoms in polymer repeat unit
N_H Number of hydrogen atoms in polymer repeat unit
N_O Number of oxygen atoms in polymer repeat unit
N_N Number of nitrogen atoms in polymer repeat unit
N_S Number of sulfur atoms in polymer repeat unit
N_{Cl} Number of chlorine atoms in polymer repeat unit
N_F Number of fluorine atoms in polymer repeat unit
N_t Total number of atoms in polymer repeat unit

The types of bonds for the repeat unit of each polymer are listed in table VI.

TABLE VI.—TYPES OF BONDS IN THE REPEAT UNIT FOR EACH MISSE 2 PEACE POLYMER

Abbreviation	N_{bO}	N_{bC}	N_{sC}	N_{dC}	N_{tC}	N_{pC}	N_{psO}	N_{pdO}	N_{pN}	N_{bN}	N_{ring}
ABS	0	8	15	12	1	15	0	0	1	0	2
CA	2	5	6	0	0	7	3	3	0	0	1
PPD–T (Kevlar)	0	14	8	6	0	0	0	2	0	2	2
PE	0	2	2	0	0	0	0	0	0	0	0
PVF (Clear Tedlar)	0	2	2	0	0	0	0	0	0	0	0
PVF (White Tedlar)	0	2	2	0	0	0	0	0	0	0	0
POM (Delrin)	1	1	0	0	0	0	0	0	0	0	0
PAN	0	2	3	0	0	1	0	0	1	0	0
ADC (CR–39)	5	12	8	2	0	0	0	2	0	0	0
PS	0	2	6	3	0	6	0	0	0	0	1
PMMA	0	2	5	0	0	3	0	0	0	0	0
PEO	1	2	1	0	0	0	0	0	0	0	0
PBO (Zylon)	2	14	8	8	0	0	0	0	0	2	4
EP	0	20	12	8	0	0	2	0	0	0	5
PP	0	2	3	0	0	1	0	0	0	0	0
PBT	2	12	8	3	0	0	0	2	0	0	1
PSU	2	25	16	12	0	2	0	2	0	0	4
PU	2	6	2	0	0	0	0	2	0	2	0
PPPA (Nomex)	0	8	8	6	0	0	0	2	0	2	2
PG	0	6	6	3	0	0	0	0	0	0	1
PEI	2	22	23	15	0	2	0	4	0	2	7
PA 6	0	6	5	0	0	0	0	1	0	1	0
PA 66	0	12	10	0	0	0	0	2	0	2	0
PI (CP1)	0	30	30	18	0	4	0	4	0	2	8
PI (Kapton H)	1	22	13	18	0	0	0	4	0	2	5
PI (Kapton HN)	1	22	14	9	0	0	0	4	0	2	5
PI (Upilex–S)	0	22	13	9	0	0	0	4	0	2	5
PI (PMR–15)	0	95	70	33	0	0	0	14	0	6	18
PBI	0	20	12	14	0	0	0	0	0	4	5
PC	2	16	10	6	0	2	0	1	0	0	2
PEEK	1	19	12	9	0	0	0	1	0	0	3
PET (Mylar)	2	10	6	3	0	0	0	2	0	0	1
CTFE (Kel–f)	0	2	2	0	0	0	0	0	0	0	0
ECTFE (Halar)	0	4	4	0	0	0	0	0	0	0	0
ETFE (Tefzel)	0	4	4	0	0	0	0	0	0	0	0
FEP	0	2	10	0	0	0	0	0	0	0	0
PTFE	0	2	2	0	0	0	0	0	0	0	0
PVDF (Kynar)	0	2	2	0	0	0	0	0	0	0	0
PFA	0	200	203	0	0	3	1	0	0	0	0
AF	0	10	16	0	0	9	6	0	0	0	3

Where

N_{bO} Number of oxygen atoms in backbone of polymer repeat unit
N_{bC} Number of carbon atoms in backbone of polymer repeat unit
N_{sC} Number of single bonded carbon atoms in polymer repeat unit
N_{dC} Number of double bonded carbon atoms in polymer repeat unit
N_{tC} Number of triple bonded carbon atoms in polymer repeat unit
N_{pC} Number of carbon atoms pendant to backbone of polymer repeat unit

N_{psO} Number of single bonded oxygen atoms pendant to backbone of polymer repeat unit
N_{pdO} Number of double bonded oxygen atoms pendant to backbone of polymer repeat unit
N_{pN} Number of nitrogen atoms pendant to backbone of polymer repeat unit
N_{bN} Number of nitrogen atoms in backbone of polymer repeat unit
N_{ring} Number of ring structures (such as benzyl and other mixed atom rings) in polymer repeat unit

For polymers containing ring structures in the backbone, all carbon atoms around each ring are considered as part of the backbone structure. The bond at either end of a typical polymer repeat unit is counted as one half of a C-C bond in cases where the adjoining bond is to a carbon atom.

2.4 Optimization of Predictive Tool Dependencies

A variety of predictive equations for LEO erosion yield were evaluated based on the chemical and physical properties listed in sections 2.1 through 2.3. Over 100 trial equations were constructed and optimized based on arguments as to what atoms and bonding were thought to influence the atomic oxygen erosion yield. The equations were then optimized and tested for the best linear fit to the actual space data from the MISSE 2 PEACE Polymer experiment. It was assumed that some bonds (such as oxygen in the backbone) contributed to causing a higher erosion yield, and that others (such as pendant fluorine atoms) caused a lower erosion yield. To take the bonding dependencies into account, an overall erosion yield dependent formula was assumed in which each bonding type dependency variable had a multiplicative constant coefficient that was multiplied by the number of atoms or bonds of each type, then summed, and then divided by the number of carbon atoms in the backbone of the polymer repeat unit. Thus, the erosion yield was made up of terms which added or subtracted from the erosion yield. Other terms such as the physical density, the packing of atoms based on the volume per repeat unit compared to the sum of the volume of covalent bonded atoms in the repeat unit, ash content, and the ratios of fluorine, chlorine, nitrogen, oxygen, and pendant carbon atoms to total atoms or carbon atoms in the repeat unit were assumed to be multiplicative terms with their own constants. The optimization of the candidate erosion yield dependency equations were performed by sequential iteration of the overall formulae's 27 constants to maximize the correlation coefficient of a linear curve fit to the observed LEO flight erosion yield data. The iterations were carried out (typically requiring 6 to 10 iterations) until the correlation coefficient changed by less than 0.1 percent. The formula for the equation with the highest correlation coefficient is given in this paper.

3.0 Results and Discussion

A predictive equation was developed by assuming that the atomic oxygen erosion yield of a polymer has a linear relationship between a unitless variable which is multiplicative combination of polymer composition, bonding, density, and ash content properties. A unitless erosion yield dependent variable, x, was defined as a weighted sum of types and number of bonds divided by the number of carbon atoms in the backbone with additional multiplicative terms. The atomic oxygen erosion yield predictive equation, which has a linear dependence on x, would be given by

$$E_y = mx + b \tag{1}$$

Where

E_y atomic oxygen erosion yield, cm^3/atom
m Slope of best fit linear equation relating the measured atomic erosion yield to the erosion yield dependent variable, x
b Y axis intercept for the best fit equation of erosion yield versus x

The general form of erosion yield dependent variable, x, which resulted in the highest correlation coefficient is shown below (the variables and constants are provided in table VI):

$$x = (C_{bO}N_{bO} + C_{bC}N_{bC} + C_H N_H + C_{sC}N_{sC} + C_{dC}N_{dC} + C_{tC}N_{tC} + C_{pC}N_{pC} + C_{pdO}N_{pdO} + C_{pN}N_{pN} + C_{bN}N_{bN} + C_S N_S + C_{Cl}N_{Cl} + C_F N_F + C_{ring}N_{ring})(1/N_{bC})(1 + C_{\Sigma/v}\, V_\Sigma/V_r)(e^{-(C_a N_a/(1-N_a))})$$
$$(1 + C_\rho \rho)(1 + C_{F/t}N_F/N_t)(1 + C_{O/C}N_O/N_C)(1 + C_{F/C}N_F/N_C)(1 + C_{H/C}N_H/N_C)$$
$$(1 + C_{N/C}N_N/N_C)(1 + C_{Cl/C}N_{Cl}/N_C)(1 + C_{pC/C}N_{pC}/N_C)(1 + C_{bC/C}N_{bC}/N_C)$$
$$(1 + C_{sC/C}N_{sC}/N_C) \qquad (2)$$

Where

C_{bO}, C_{bC}, C_H, C_{sC}, C_{dC}, C_{tC}, C_{pC}, C_{psO}, C_{pdO}, C_{pN}, C_{bN}, C_S, C_{Cl}, C_F, C_{ring}, $C_{\Sigma/v}$, C_a, C_ρ, $C_{F/t}$, $C_{O/C}$, $C_{F/C}$, $C_{H/C}$, $C_{N/C}$, $C_{Cl/C}$, $C_{pC/C}$, $C_{bC/C}$, and $C_{sC/C}$ are constants associated with the various terms relating to the number of atoms, bonds, or physical characteristics of the polymers including the parameters listed in section 2.3. The first 14 products of constants and number of bonds or atoms are added together and divided by the number of backbone carbon atoms, N_{bC}, to normalize the effects of these terms relative to the backbone length.

The first additional multiplicative term is the ratio of the sum of the volume of atoms in the repeat unit (based on their covalent radii) (V_Σ), to the volume of the repeat unit (V_r), times a constant, $C_{\Sigma/v}$. This ratio represents how close the atoms of the repeat unit are packed to what they could be if there was no void space in the polymer.

The next multiplicative term attempts to take into account the effect on erosion yield caused by the mass fraction of the polymer that is ash, N_a. It uses an exponential relationship and a constant to produce a decreasing erosion yield with increasing ash content. The ash content term:

$$(e^{-(C_a N_a/(1-N_a))})$$

was designed to produce an erosion yield of zero if the ash content was one and a finite erosion yield if the ash content was zero.

The next multiplicative factor allows for adjustment of the erosion yield based on the density of the polymer times a constant.

The last nine multiplicative terms take into account the ratios of fluorine, chlorine, nitrogen, oxygen, single bonded carbon, pendant carbon, and backbone carbon atoms to either total atoms or carbon atoms in the repeat unit. The number one added to these ratios allows the formula to produce meaningful results even if there are no atoms or bonds of a particular type.

By making plots of x using the physical and chemical properties and erosion yields listed in the preceding tables, one could optimize the various constants to maximize the correlation coefficient of a linear fit between x and the measured erosion yields as shown in figure 5.

Based on the linear equation for the best fit line shown in figure 5, the resulting predicted atomic oxygen erosion yield, E_y, in cm^3/atom is simply given by equation (1) where the definition and values for the variables and constants are given in table VI.

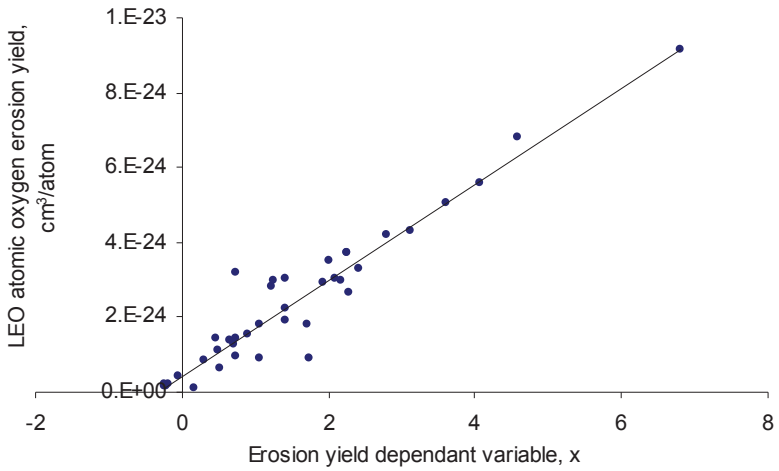

Figure 5.—Optimized linear fit between the LEO MISSE 2 PEACE atomic oxygen erosion yields and the erosion yield dependant variable, *x*, which results in a correlation coefficient of 0.914.

TABLE VI.—DEFINITION AND VALUES OF VARIABLES AND CONSTANTS

Symbol	Definition	Value
m	Slope of best fit linear equation relating the measured atomic erosion yield to the erosion yield dependent variable, x	1.28×10^{-24} cm^3/atom
b	Y axis intercept in figure 4 for the best fit equation	4.44×10^{-25} cm^3/atom
C_{bO}	Constant for oxygen atoms in backbone of polymer repeat unit	1.7
C_H	Coefficient constant of hydrogen atoms in polymer repeat unit	4.1
C_{bC}	Constant for carbon atoms in backbone of polymer repeat unit	1.52
C_{sC}	Constant for single bonded carbon atoms in polymer repeat unit	–1.57
C_{dC}	Constant for double bonded carbon atoms in polymer repeat unit	–1.9
C_{tC}	Constant for triple bonded carbon atoms in polymer repeat unit	–43
C_{pC}	Constant for carbon atoms pendant to backbone of polymer repeat unit	0.2
C_{psO}	Constant for single bonded oxygen atoms pendant to backbone of polymer repeat unit	–3.1
C_{pdO}	Constant for double bonded oxygen atoms pendant to backbone of polymer repeat unit	–8.9
C_{pN}	Constant for nitrogen atoms pendant to backbone of polymer repeat unit	–4.1
C_{bN}	Constant for nitrogen atoms in backbone of polymer repeat unit	–13
C_S	Constant for sulfur atoms in polymer repeat unit	–26
C_{Cl}	Constant for chlorine atoms in polymer repeat unit	6.6
C_F	Constant for fluorine atoms in polymer repeat unit	–0.33
C_{ring}	Constant for number of rings in polymer repeat unit	15.6
$C_{\Sigma/v}$	Constant for ratio of sum of volume of atoms in repeat unit (based on their covalent radii) to volume of the repeat unit	–6.55
C_a	Constant for mass fraction of polymer that is ash	5.8
C_ρ	Constant for polymer density	0.64 cm^3/gram
$C_{F/t}$	Constant for the ratio of the fluorine atoms to total atoms in the repeat unit	–1.23
$C_{O/C}$	Constant for the ratio of oxygen atoms to carbon atoms in the repeat unit	2.31
$C_{F/C}$	Constant for the ratio of the fluorine atoms to carbon atoms in the repeat unit	–0.04
$C_{H/C}$	Constant for the ratio of the hydrogen atoms to carbon atoms in the repeat unit	–0.317
$C_{N/C}$	Constant for the ratio of the nitrogen atoms to carbon atoms in the repeat unit	2.3
$C_{Cl/C}$	Constant for the ratio of the chlorine atoms to carbon atoms in the repeat unit	–1.2
$C_{pC/C}$	Constant for the ratio of pendant carbon atoms to carbon atoms in the repeat unit	–0.82
$C_{bC/C}$	Constant for the ratio of repeat unit backbone carbon atoms to total carbon atoms in the repeat unit	0.54
$C_{sC/C}$	Constant for the ratio of the single bonded carbon atoms to total carbon atoms in the repeat unit	0.82

The above atomic oxygen erosion yield predictive formula has a correlation coefficient of 0.914 for its fit to the space data from the 38 MISSE 2 PEACE polymers and graphite. Only one polymer, polyethylene oxide (PEO), was found to be significantly off the linear fit. The measured space erosion yield appeared to be anomalously low by a factor of greater than three in comparison with the predictive formula. Inclusion of the PEO data resulted in a significant reduction in the correlation coefficient. As a result, the PEO erosion yield value was not used for the formulation of the atomic oxygen erosion yield predictive tool data base. As more in-space data becomes available, variations to this formula, and the development of new formulas, will be possible, which have improvements that produce a higher level of correlation.

Figure 6 and table VII compare the resulting predicted atomic oxygen erosion yield with all the measured MISSE 2 materials with the exception of PEO. The linear curve of figure 6 has a correlation coefficient of 0.914.

One data point that tends to validate this predictive tool is that using this predictive tool for diamond produces a negative predicted atomic erosion yield (-1×10^{-22} cm^3/atom) indicating the carbon atoms in diamond are sufficiently close together to result in shielding caused by oxygen that bonds on to the surface of the diamond which prevents further atomic oxygen reaction. Thus, diamond should not erode in a LEO atomic oxygen environment. Space results and laboratory testing have previously validated this prediction (ref. 6).

The ash content does play an important role in protecting polymers in LEO as can be seen by comparing the erosion yields of clear and white PVF (Tedlar). However, thin polymers that eroded faster at their perimeter where atomic oxygen focusing from the chamfered aluminum holders occurred could peel up resulting in an ash is only partially covering the surface below it (ref. 19). Thus, the effectiveness of ash protection can potentially be reduced if the polymers are thin and erode completely through in a manner that removes the protecting ash. This, of course, complicates erosion yield prediction.

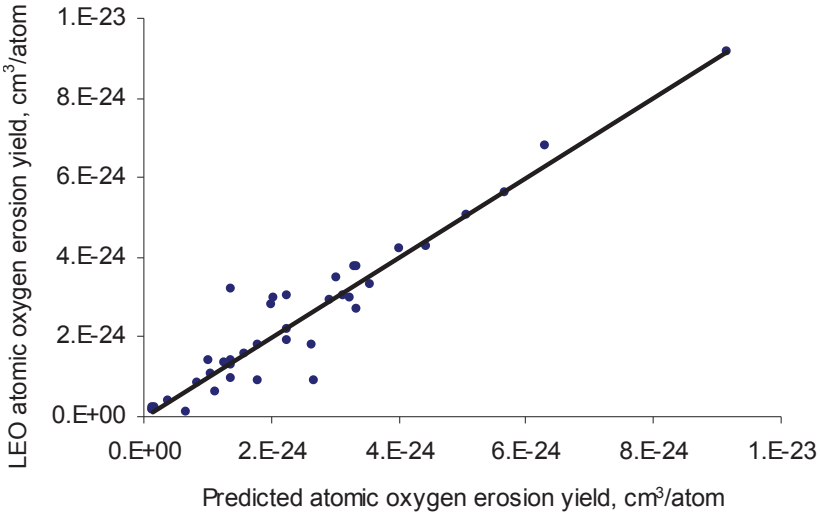

Figure 6.—Compares the resulting atomic predicted atomic oxygen erosion yield with the measured MISSE 2 PEACE polymers including pyrolytic graphite (with the exception of PEO).

TABLE VII.—COMPARISON OF THE PREDICTED AND ACTUAL MEASURED ATOMIC OXYGEN EROSION YIELDS

Material	Polymer abbreviation	Predicted erosion yield, cm^3/atom	MISSE 2 erosion yield, cm^3/atom
Acrylonitrile butadiene styrene	ABS	1.07×10^{-24}	1.09×10^{-24}
Cellulose acetate	CA	5.06×10^{-24}	5.05×10^{-24}
Poly-(p-phenylene terephthalamide)	PPD–T (Kevlar)	1.12×10^{-24}	6.28×10^{-25}
Polyethylene	PE	3.32×10^{-24}	$>3.74\times10^{-24}$
Polyvinyl fluoride - clear	PVF (Tedlar)	1.38×10^{-24}	3.19×10^{-24}
Polyvinylfluoride with white pigment	PVF (White Tedlar)	6.61×10^{-24}	1.01×10^{-25}
Polyoxymethylene; acetal; polyformaldehyde	POM (Delrin)	9.14×10^{-24}	9.14×10^{-24}
Polyacrylonitrile	PAN	1.37×10^{-24}	1.41×10^{-24}
Allyl diglycol carbonate	ADC (CR–39)	6.30×10^{-24}	$>6.80\times10^{-24}$
Polystyrene	PS	3.33×10^{-24}	3.74×10^{-24}
Polymethyl methacrylate	PMMA	5.65×10^{-24}	$>5.60\times10^{-24}$
Polyethylene oxide	PEO	7.99×10^{-24}	1.93×10^{-24}
Poly(p-phenylene-2 6-benzobisoxazole)	PBO (Zylon)	1.28×10^{-24}	1.36×10^{-24}
Epoxide or epoxy	EP	4.02×10^{-24}	4.21×10^{-24}
Polypropylene	PP	3.36×10^{-24}	2.68×10^{-24}
Polybutylene terephthalate	PBT	2.68×10^{-24}	9.11×10^{-25}
Polysulphone	PSU	2.92×10^{-24}	2.94×10^{-24}
Pol yurethane	PU	1.58×10^{-24}	1.56×10^{-24}
Polyphenylene isophthalate	PPPA (Nomex)	1.03×10^{-24}	1.41×10^{-24}
Pyrolytic graphite	PG	3.73×10^{-25}	4.15×10^{-25}
Polyetherimide	PEI	3.54×10^{-24}	$>3.31\times10^{-24}$
Polyamide 6 or nylon 6	PA 6	3.02×10^{-24}	3.51×10^{-24}
Polyamide 66 or nylon 66	PA 66	2.62×10^{-24}	1.80×10^{-24}
Polyimide	PI (CP1)	2.27×10^{-24}	1.91×10^{-24}
Polyimide (PMDA)	PI (Kapton H)	2.06×10^{-24}	3.00×10^{-24}
Polyimide (PMDA)	PI (Kapton HN)	2.01×10^{-24}	2.81×10^{-24}
Polyimide (BPDA)	PI (Upilex–S)	1.81×10^{-24}	9.22×10^{-25}
High temperature polyimide resin	PI (PMR–15)	2.27×10^{-24}	$>3.02\times10^{-24}$
Polybenzimidazole	PBI	2.27×10^{-24}	$>2.21\times10^{-24}$
Polycarbonate	PC	4.42×10^{-24}	4.29×10^{-24}
Polyetheretherkeytone	PEEK	4.24×10^{-24}	2.99×10^{-24}
Polyethylene terephthalate	PET (Mylar)	3.12×10^{-24}	3.01×10^{-24}
Chlorotrifluoroethylene	CTFE (Kel–f)	8.37×10^{-25}	8.31×10^{-25}
Ethylene-chlorotrifluoroethylene	ECTFE (Halar)	1.80×10^{-24}	1.79×10^{-24}
Tetrafluorethylene-ethylene copolymer	ETFE (Tefzel)	1.39×10^{-24}	9.61×10^{-25}
Fluorinated ethylene propylene	FEP	1.25×10^{-26}	2.00×10^{-25}
Polytetrafluoroethylene	PTFE	1.58×10^{-25}	1.42×10^{-25}
Perfluoroalkoxy copolymer resin	PFA	1.32×10^{-24}	1.73×10^{-25}
Amorphous fluoropolymer	AF	1.90×10^{-25}	1.98×10^{-25}
Polyvinylidene fluoride	PVDF (Kynar)	1.36×10^{-25}	1.29×10^{-24}

Summary

A predictive tool was developed to estimate the LEO atomic oxygen erosion yield of polymers based on the results of the MISSE 2 PEACE Polymers experiment, which accurately measured the erosion yield of a wide variety of polymers and pyrolytic graphite. The materials tested were selected specifically to represent a variety of polymers used in space as well as a wide variety of polymer chemical structures. The predictive tool utilizes the chemical structure, bonding information and physical properties (such as density and ash content) that can be measured in ground laboratory tests to develop an equation which predicts the space atomic oxygen erosion yield. The resulting predictive tool has a correlation coefficient of 0.914 when compared with actual MISSE 2 PEACE Polymers space data (for 38 polymers and pyrolytic graphite). One polymer, polyethylene oxide (PEO), was found to be significantly off the linear

fit for some unknown reason and was not used in the predictive tool equation. The predictive tool does predict that the diamond should not erode in LEO atomic oxygen as has been experimentally observed. The atomic oxygen erosion predictive tool allows reasonable estimates of the in-space atomic oxygen erosion yields based on chemical and physical properties as well as low cost RF plasma asher testing. The intent of the predictive tool is to be able to make estimates of LEO atomic oxygen erosion yields for new polymers without requiring expensive and time consumptive in-space testing.

References

1. Leger, L.J., Spiker, I.K., Kuminecz, J.F., Ballentine, T.J., and Visentinem, J.T., "STS Flight 5 LEO Effects Experiment—Background and Description of Thin Film Results," AIAA–83–2631–CP, October, 1983.
2. Smith, K.A., "Evaluation of Oxygen Interaction With Materials (EOIM)—STS–8, Atomic Oxygen Effects, AIAA–85–7021, November, 1985.
3. Banks, B.A., Mirtich, M.J., Rutledge, S.K., and Nahra, H.K., "Protection of Solar Array Blankets from Attack by Low Earth Orbital Atomic Oxygen," presented at the 18th IEEE Photovoltaic Specialists Conference, Las Vegas, Nevada, October 21–25, 1985.
4. Banks, B.A., Mirtich, M.J., Rutledge, S.K., and Swec, D.M., "Sputtered Coatings for Protection of Spacecraft Polymers," presented at the 11th International Conference on Metallurgical Coatings (ICMC), San Diego, California, April 9–13, 1984; published in Thin Solid Films, 127, 1985.
5. Banks, B.A. and Rutledge, S.K., "Low Earth Orbital Atomic Oxygen Simulation for Materials Durability Evaluation," Proceedings of the 4th European Symposium on Spacecraft Materials in Space Environment, Toulouse, FRANCE, September 6–9, 1988.
6. B.A. Banks, "The Use of Fluoropolymers in Space Applications" in *Modern Fluoropolymers*, Edited by John Scheirs, Chapter 4 (pp. 103–113), John Wiley & Sons Ltd, 1997.
7. ASTM E 2089–00, "Standard Practices for Ground Laboratory Atomic Oxygen Interaction Evaluation of Materials for Space Applications, June 2000.
8. Slemp, W.S., Santos-Mason, B., Bykes, G.F., Jr., and Witte, W.S., Jr., "Effects of STS–8 Atomic Oxygen Exposure on Composites, Polymeric Films and Coatings," AIAA–85–0421, January, 1985.
9. Silverman, E., "Space Environmental Effects on Spacecraft LEO Materials Selection Guide," NASA Contractor Report 4661, August 1995.
10. Koontz, S.L., Leger, L.J., Rickman, S.L., Hakes, C.L., Bui, D.T., Hunton, D.E., and Cross, J.B., "Oxygen Interactions with Materials III—Mission and Induced Environments," Journal of Spacecraft and Rockets, Vol. 32, No. 3, May—June 1995.
11. de Groh, K., Banks, B., McCarthy, C., Berger, L., and Roberts, L., "Analysis of the MISSE PEACE Polymers International Space Station Environmental Exposure Experiment," Paper presented at the 10th International Symposium on Materials in a Space Environment & 8th International Conference on Protection of Materials and Structures in a Space Environment, Collioure, France, June 19–23, 2006.
12. de Groh, K., Banks, B., McCarthy, Rucker, R., Roberts, L., and Berger, L., "MISSE PEACE Polymers Atomic Oxygen Erosion Results," NASA/TM—2006-214482, November, 2006.
13. Integrity Testing Laboratory, Inc., "Prediction of Erosion of Polymer-Based Materials by Atomic Oxygen in LEO," NASA Contract Report #C–72917–G, 1998.
14. Kleiman, J., Iskanderova, Z., Banks, B.A., de Groh, K.K., and Sechkar, E., "Prediction and Measurement of the Atomic Oxygen Erosion Yield of Polymers in Low Earth Orbital Flight," proceedings of the 8th International Symposium on Materials in a Space Environment and the 5th International Conference on Protection of Materials and Structures from the LEO Space Environment cosponsored by the CNES, Integrity Testing Laboratory, ESA, ONERA and the Canadian Space Agency, Arcachon, France, June 4–9, 2000.

15. Minton, D.J., Stockdale, D.P., Lee, D., Yu, L., and Minton, T., "Probing the Effects of Molecular Structure on the Erosion of Hydrocarbon-Based Polymers by Atomic Oxygen," Proceedings of the 10th International Symposium on Materials in a Space Environment & 8th International Conference on Protection of Materials and Structures in a Space Environment, Collioure, France, June 19–23, 2006.
16. Miller, S.K., Banks, B.A., Waters, D.L., "Investigation into the Differences in Atomic Oxygen Erosion Yields of Materials in Ground Based Facilities Compared to Those in LEO," Proceedings of the 6th International Symposium on Materials in a Space Environment & 8th International Conference on Protection of Materials and Structures in a Space Environment, Collioure, France, June 19–23, 2006.
17. Pippin, G. and Normand, E. "Estimated Environmental Exposures for MISSE–1 and MISSE–2," Proceedings of the 1st MISSE Post-Retrieval Conference, June 26–30, 2006, Orlando, FL.
18. Dever, J.A., Miller, S.K., Sechkar, E.A, and Wittberg, T.N., "Preliminary Analysis of Polymer Film Thermal Control and Gossamer Materials Experiments on Materials International Space Station Experiment (MISSE 1 and MISSE 2)," in proceedings of the 2006 MISSE Post-Retrieval Conference sponsored by the Air Force Research Laboratory, Orlando, Florida, June 26–30, 2006.
19. Banks, B.A., de Groh, K.K., Miller, S.K., and Waters, D.L., "Lessons Learned from Atomic Oxygen Interaction with Materials in Low Earth Orbit," NASA/TM—2008-215264 July 2008, Paper presented at the 9th International Conference on Protection of Materials and Structures in a Space Environment, Toronto, Canada, May 20–23, 2008.

Appendix A—Chemical Structure of MISSE 2 PEACE polymers

Acrylonitrile Butadiene Styrene
ABS
$C_{23}H_{23}N$

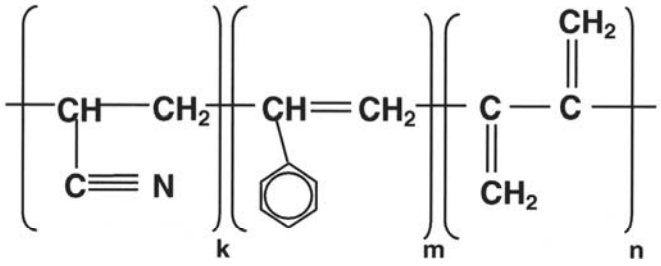

k = 1
m = 2
n = 1

Cellulose Acetate
CA
$C_{12}H_{16}O_8$

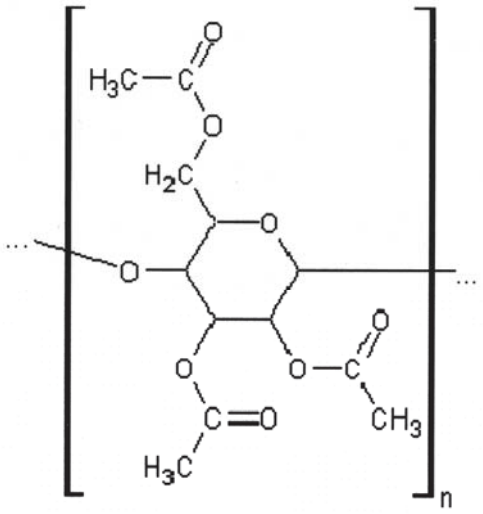

Poly(p-phenylene terephthalamide)
PPD-T – Kevlar
$C_{14}H_{10}N_2O_2$

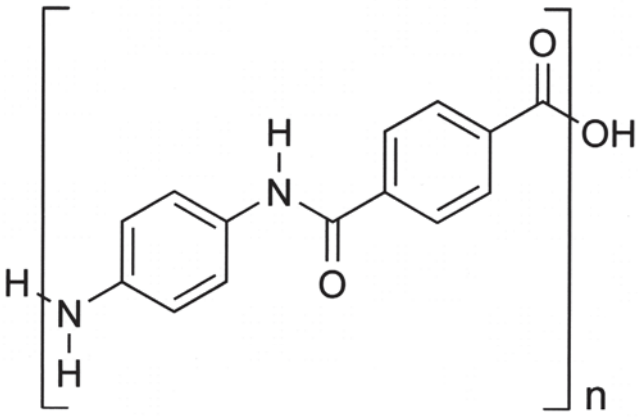

Polyethylene
PE
C_2H_4

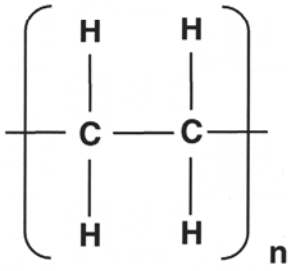

Polyvinl Fluoride
PVF (Tedlar)
C_2H_3F

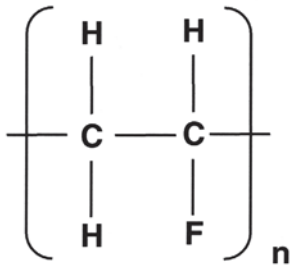

Polyoxymethylene
POM – Delrin,
CH_2O

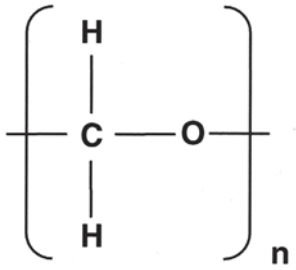

Polyacrylonitrile
PAN
C_3H_3N

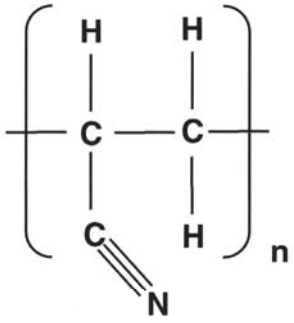

Ally Diglycol Carbonate
ADC
CR-39
$C_{12}H_{18}O_7$

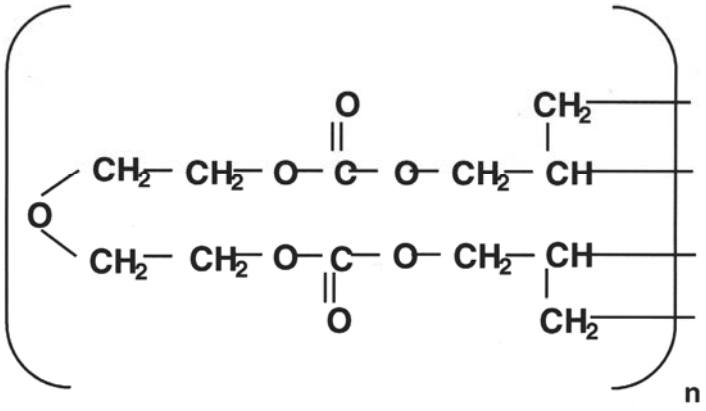

Polystyrene
PS
C_8H_8

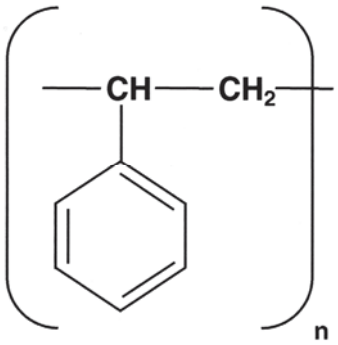

Polymethylmethacrylate
PMMA
$C_5H_8O_2$

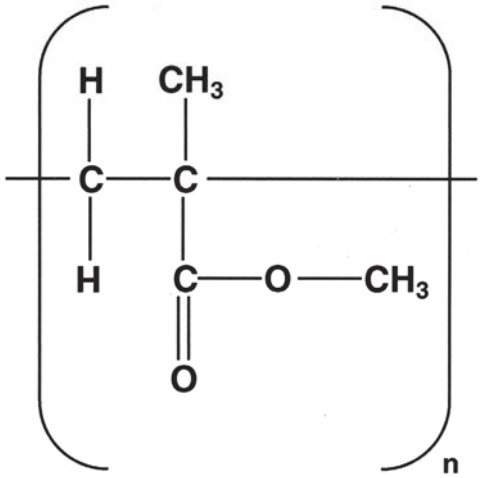

Polyethylene oxide
PEO
C_2H_4O

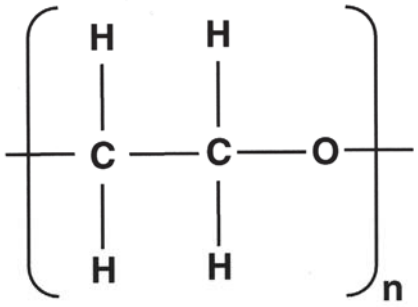

Poly(p-phenylene-2,6-benzobisoxazole)
PBO (Zylon)
$C_{14}H_6O_2N_2$

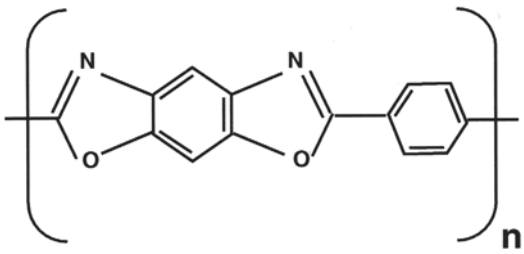

Epoxy
EP
$C_{20}H_{19}O_3$

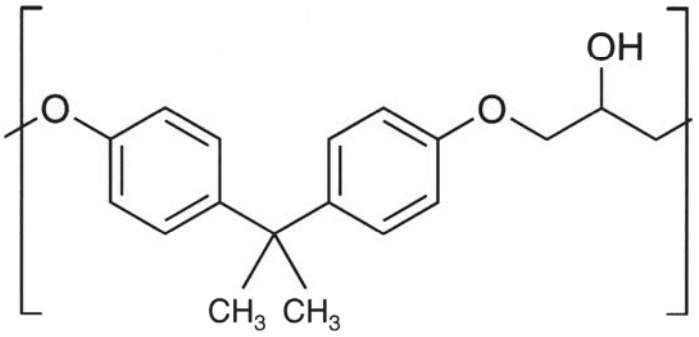

Polypropylene
PP
C_3H_6

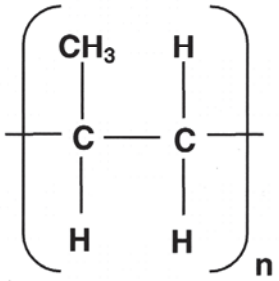

Polybutylene terephthalate
PBT
$C_{12}H_{12}O_4$

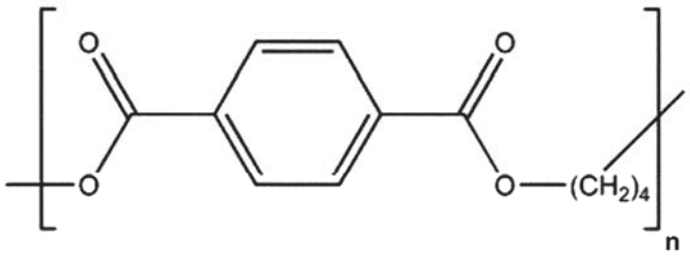

Polysulphone
PSU
$C_{27}H_{22}O_4S$

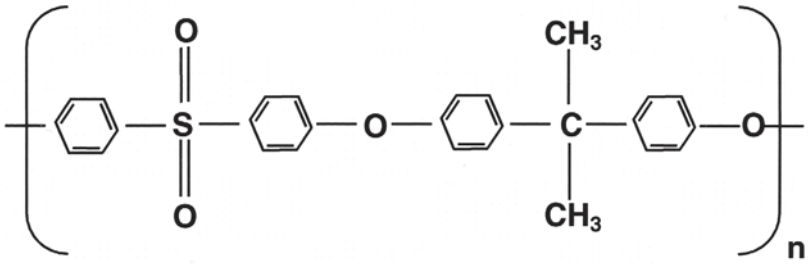

Polyurethane
PU
$C_6H_{10}O_4N_2$

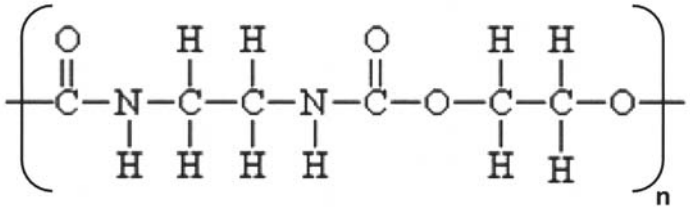

Polyethylene Isophthalate
PPPA (Nomex)
$C_{14}H_{10}O_2N_2$

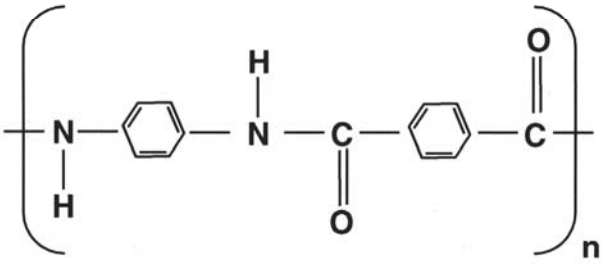

Pyrolytic graphite
PG
C_6

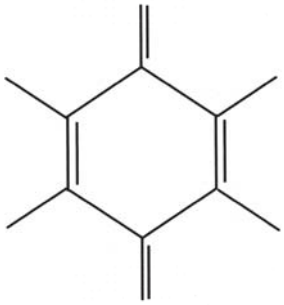

Polyetherimide
PEI
$C_{37}H_{24}O_6N_2$

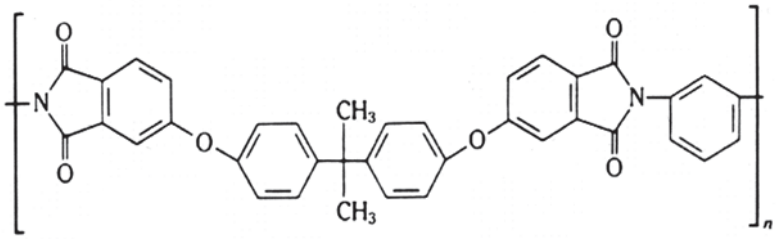

Polyamide
PA 6 (Nylon 6)
$C_6H_{11}ON$

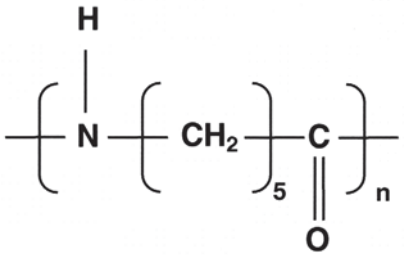

Polyamide
PA 66 (Nylon 6,6)
$C_{12}H_{22}O_2N_2$

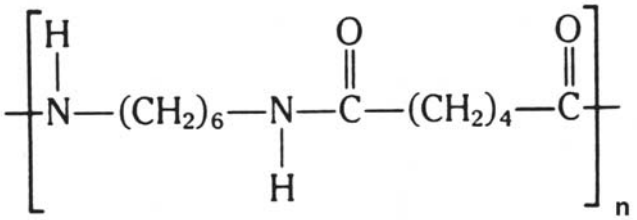

Polyimide
CP-1
$C_{46}H_{22}O_5N_2F_6$

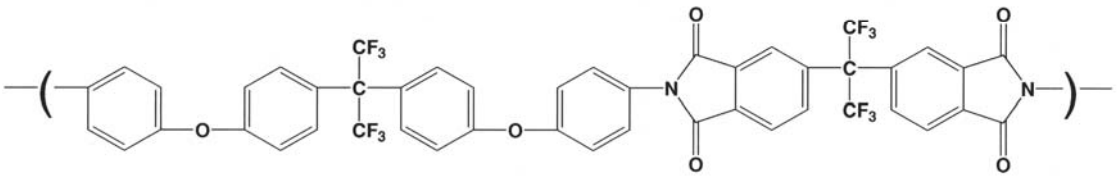

Polyimide
PI (Kapton H or HN)
$C_{22}H_{10}O_5N_2$

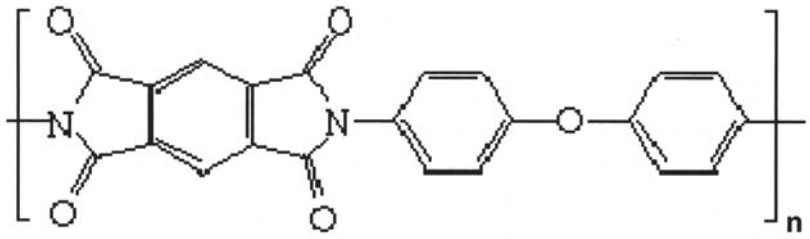

Polyimide (PMDA)
Upilex-S
$C_{22}H_{10}O_4N_2$

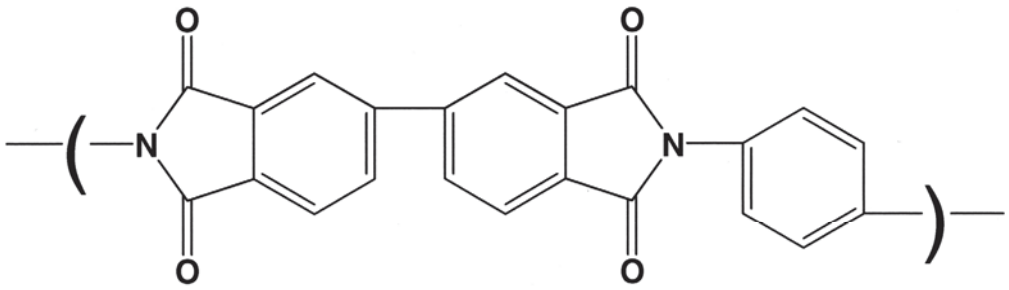

High Temperature Polyimide Resin
PMR-15
$C_{95}H_{57}O_{14}N_6$

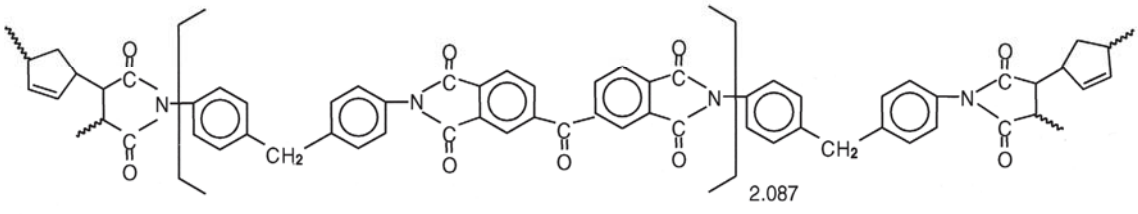

Polybenzimidazole
PBI
$C_{20}H_{12}N_4$

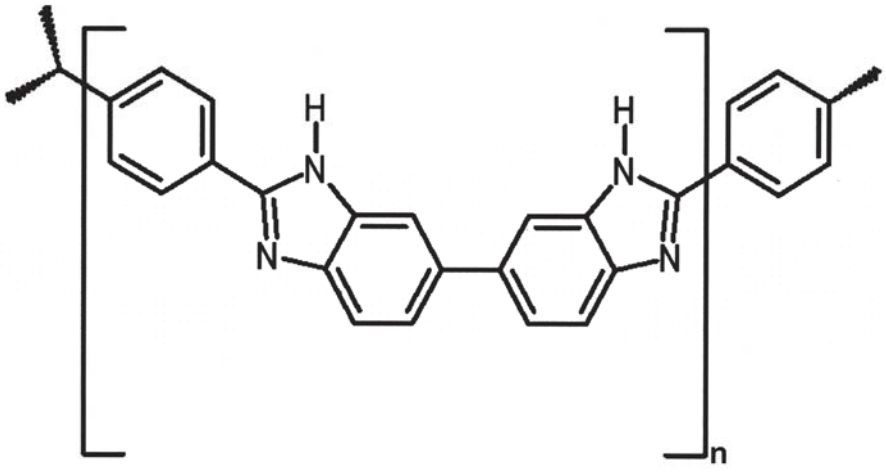

Polycarbonate
PC
$C_{16}H_{14}O_3$

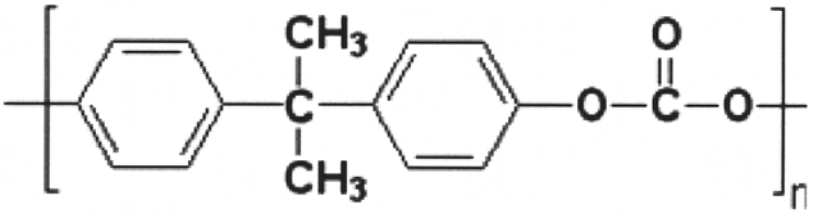

Polyether Ether Keytone
PEEK
$C_{19}H_{12}O_2$

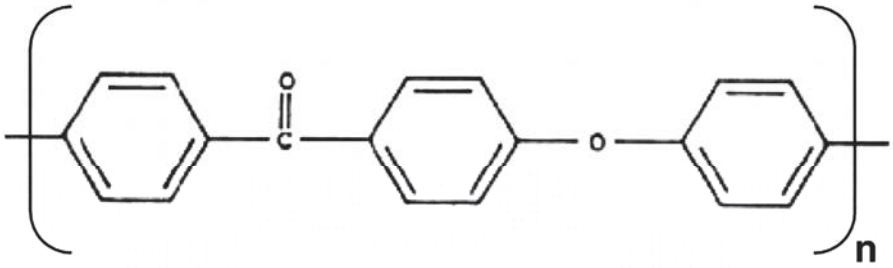

Polyethylene Terephthalate
PET
$C_{10}H_8O_4$

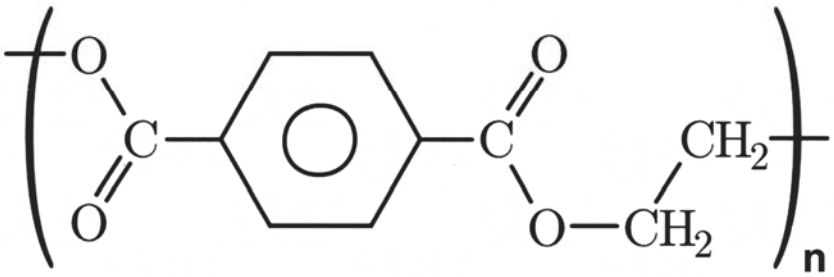

Chlorotrifluoroethylene
CTFE (Kel-f)
C_2ClF_3

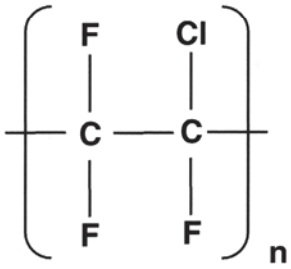

Ethylene-chlorotri-ethylene Copolymer
ECTFE (Halar)
$C_4H_4F_3Cl$

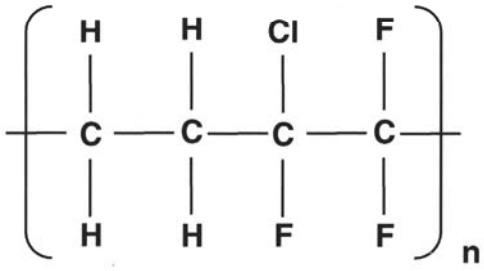

Tetrafluoroethylene-ethylene Copolymer
ETFE (Tefzel)
$C_4H_4F_4$

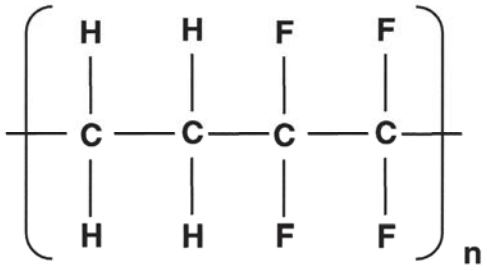

Fluorinated Ethylene Propylene
FEP
$C_{10}F_{20}$

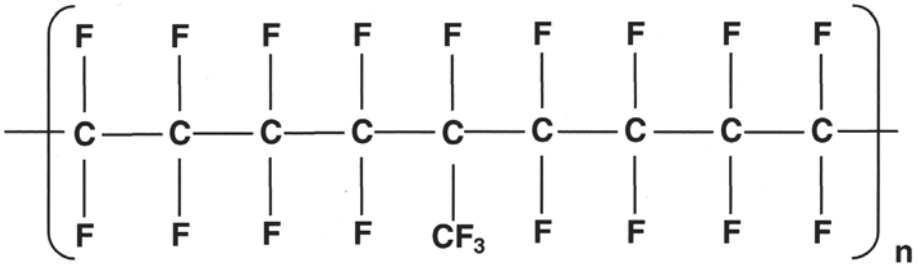

Polytetrafluoroethylene
PTFE
C_2F_4

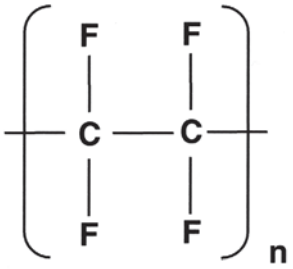

Polyvinylidene Fluoride
PVDF (Kynar)
$C_2H_2F_2$

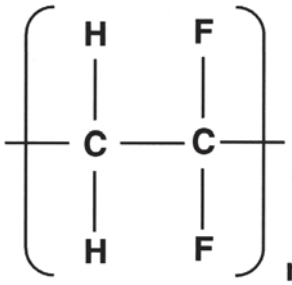

Polyfluoroalkoxy Copolymer
PFA
$C_{203}F_{406}O$

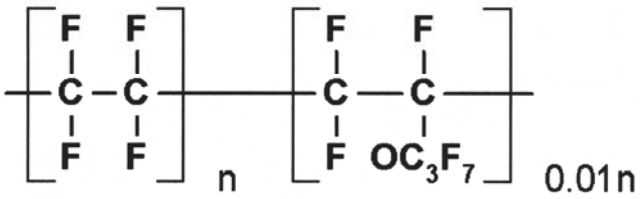

2,2-Bistrifluoromethyl-4,5difluoro-1,3-dioxole (PDD)
and Fluorine Containing Monomer
Teflon AF
$C_{19}O_6F_{32}$

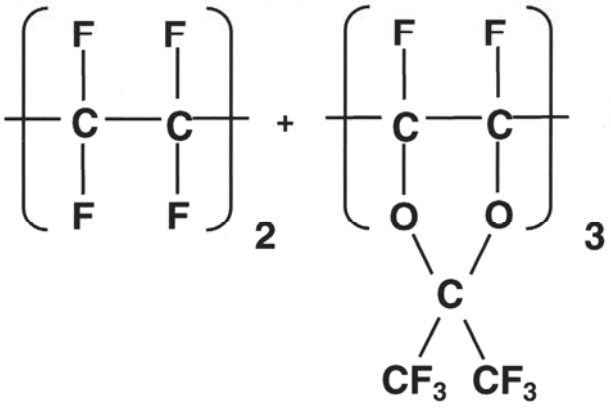

REPORT DOCUMENTATION PAGE		Form Approved OMB No. 0704-0188

1. REPORT DATE *(DD-MM-YYYY)*	2. REPORT TYPE	3. DATES COVERED *(From - To)*
01-12-2008	Technical Memorandum	

4. TITLE AND SUBTITLE
Atomic Oxygen Erosion Yield Predictive Tool for Spacecraft Polymers in Low Earth Orbit

5a. CONTRACT NUMBER

5b. GRANT NUMBER

5c. PROGRAM ELEMENT NUMBER

6. AUTHOR(S)
Banks, Bruce, A.; Backus, Jane, A.; de Groh, Kim, K.

5d. PROJECT NUMBER

5e. TASK NUMBER

5f. WORK UNIT NUMBER
WBS 659877.02.03.0672.01

7. PERFORMING ORGANIZATION NAME(S) AND ADDRESS(ES)
National Aeronautics and Space Administration
John H. Glenn Research Center at Lewis Field
Cleveland, Ohio 44135-3191

8. PERFORMING ORGANIZATION REPORT NUMBER
E-16694

9. SPONSORING/MONITORING AGENCY NAME(S) AND ADDRESS(ES)
National Aeronautics and Space Administration
Washington, DC 20546-0001

10. SPONSORING/MONITORS ACRONYM(S)
NASA

11. SPONSORING/MONITORING REPORT NUMBER
NASA/TM-2008-215490

12. DISTRIBUTION/AVAILABILITY STATEMENT
Unclassified-Unlimited
Subject Categories: 23 and 27
Available electronically at http://gltrs.grc.nasa.gov
This publication is available from the NASA Center for AeroSpace Information, 301-621-0390

13. SUPPLEMENTARY NOTES

14. ABSTRACT
A predictive tool was developed to estimate the low Earth orbit (LEO) atomic oxygen erosion yield of polymers based on the results of the Polymer Erosion and Contamination Experiment (PEACE) Polymers experiment flown as part of the Materials International Space Station Experiment 2 (MISSE 2). The MISSE 2 PEACE experiment accurately measured the erosion yield of a wide variety of polymers and pyrolytic graphite. The 40 different materials tested were selected specifically to represent a variety of polymers used in space as well as a wide variety of polymer chemical structures. The resulting erosion yield data was used to develop a predictive tool which utilizes chemical structure and physical properties of polymers that can be measured in ground laboratory testing to predict the in-space atomic oxygen erosion yield of a polymer. The properties include chemical structure, bonding information, density and ash content. The resulting predictive tool has a correlation coefficient of 0.914 when compared with actual MISSE 2 space data for 38 polymers and pyrolytic graphite. The intent of the predictive tool is to be able to make estimates of atomic oxygen erosion yields for new polymers without requiring expensive and time consumptive in-space testing.

15. SUBJECT TERMS
Atomic oxygen; Low Earth orbit; Spacecraft polymers

16. SECURITY CLASSIFICATION OF:			17. LIMITATION OF ABSTRACT	18. NUMBER OF PAGES	19a. NAME OF RESPONSIBLE PERSON
a. REPORT	b. ABSTRACT	c. THIS PAGE			STI Help Desk (email:help@sti.nasa.gov)
U	U	U	UU	43	19b. TELEPHONE NUMBER *(include area code)* 301-621-0390